Engineering Notes

ENGINEERING NOTES are short manuscripts describing new developments or important results of a preliminary nature. These Notes cannot exceed 6 manuscript pages and 3 figures; a page of text may be substituted for a figure and vice versa. After informal review by the editors, they may be published within a few months of the date of receipt. Style requirements are the same as for regular contributions (see inside back cover).

Tether Static Shape for Rotating Multimass, Multitether, Spacecraft for "Triangle" Michelson Interferometer

Anthony B. DeCou*
Northern Arizona University, Flagstaff, Arizona

Background and Summary

ONE promising method of creating an orbiting stellar interferometer is by locating three collimating telescopes at the corners of an equilateral triangle and connecting them by three tethers along the sides of the triangle.[1,2] This assembly spins slowly around an axis in the direction of observation. Centrifugal force keeps the tethers taut. Thus, by changing the length of the tethers, the separation distance of the sampling telescopes can be varied. At each telescope, the sampled radiation is split into two beams, which are sent in the direction of the other two telescopes. A fringe detector attached to each telescope receives radiation from the other two so that three baselines separated by 120 deg are sampled simultaneously by the system. A Fourier transform of the image in the direction of observation is built up gradually as the baselines rotate and the separation distance is varied.[3]

The practicality of this scheme depends on one's ability to control the positions and the angular orientation of the three telescopes, with the precision required for this type of observation. The optical path lengths of the beams must be equal to within a small fraction of a wavelength and the pointing errors must be close to the accuracy of the Hubble Space Telescope.

The following is a small but significant first step in this effort. The static shape of the tether with finite mass density is determined under the influence of the centrifugal forces caused by the rotation and in the absence of any disturbing dynamic forces such as gravity gradients, solar radiation pressure, and thermal expansion forces. The dynamic effects of these forces will be addressed next as perturbations from the static shape. The static problem has been solved by first deriving nonlinear differential equations relating the position of each tether point to the tension at each point. A numerical solution to these equations is then outlined, and the results of a computer program based on this method are summarized.

The solution has been generalized to include the cases of three equal masses M_1 and three equal tethers (see Fig. 1a) and the case in which three more equal masses M_2, not necessarily equal to M_1, are added midway between the M_1 masses, as shown in Fig. 1b.

Theoretical Foundation

Before addressing the general problem, it is instructive to consider two extreme cases. First, if the mass density of the tether is zero, there will be no centrifugal forces on the tethers, tending to bow them out; therefore, they will be stretched tight into straight lines. Second, if the corner masses are zero and the mass density of the tethers is finite, symmetry requires that the tethers assume a circular shape corresponding to maximum bowing.

The intermediate and realistic case corresponding to finite point masses at the corners and finite mass density of the tethers can be handled as follows. First, define a polar coordinate system centered at the center of gravity of the system (assumed to be at equilibrium) and rotating around the same axis as the system with the same angular velocity ω. Let θ be the angle measured from a radial line extending through the center of one of the tethers as shown in Fig. 1a. A three-mass system has been chosen for purposes of illustration. Let $R(\theta)$ be the radial distance to the tether and $T(\theta)$ the tension force in the tether. By symmetry, it is clear that the shape of the entire system is determined by $R(\theta)$ in the range $0 \le \theta \le \pi/3$ rad.

Also note the effect of inserting an equal number of different-sized masses M_2 midway between the three masses of Fig. 1a, as shown in Fig. 1b. The shape will change but the symmetry around the horizontal axis remains, and the shape of the entire configuration is still determined uniquely by $R(\theta)$ in the range $0 \le \theta \le \pi/3$.

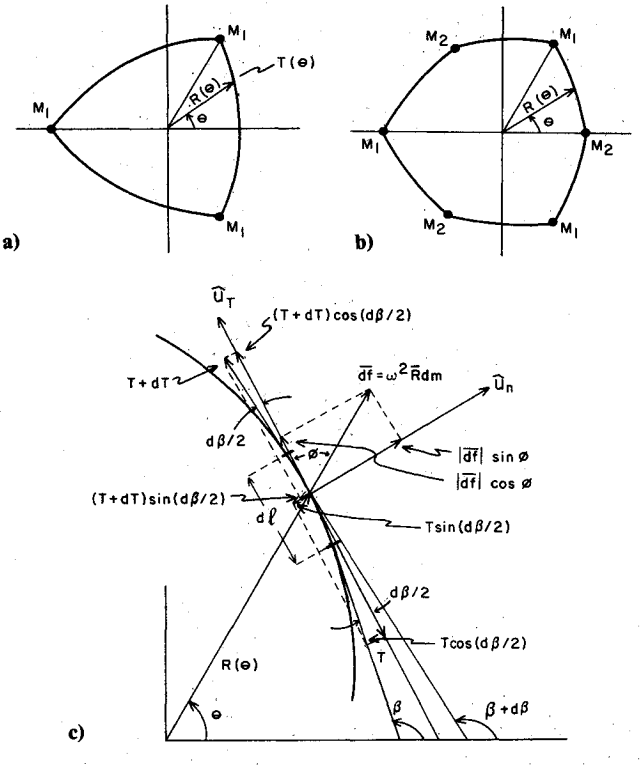

Fig. 1 a) Basic triangular configuration; b) with point secondary masses M_2 included; and c) a differential segment of the tether of length $d\ell$ showing all of the vector forces acting on the segment and the components of these forces tangent to the segment and normal to the segment at equilibrium.

Received Oct. 22, 1987; revision received Feb. 29, 1988.

*Assistant Professor, College of Engineering.

The differential equations relating $R(\theta)$ and the tension $T(\theta)$ are derived with the help of Fig. 1c. The tension force vector must be tangent to the tether at every point because it is assumed that the tether cannot sustain any shear stress. A differential segment of the tether $d\ell$ is shown with tension forces T and $T + dT$ pulling on both ends of it in "nearly" opposite directions. These tangent directions make angles β and $\beta + d\beta$ with the horizontal axis of the coordinate system as shown. The centrifugal force acting on the differential segment is shown pointing radially away from the center of rotation, which is the origin of the polar coordinate system. The magnitude of this force is $\omega^2 R\, dm$, where ω is the constant rate of rotation of the system in radians per second and R the radial distance of the differential mass dm from the origin.

An orthogonal coordinate system is established with its origin at the center of the differential segment and with its two unit vectors $\hat{U}_T$ and $\hat{U}_n$ tangent to the tether and normal to the tether at that point as shown. The angle between the tangent direction and the radial direction to the differential segment is ϕ, and the angles between the tangent direction and the two tension forces is $d\beta/2$. At equilibrium, the forces on the differential segment in any direction must sum to zero. Writing a force balance in the $\hat{U}_T$ direction gives

$$T\cos(d\beta/2) - (T + dT)\cos(d\beta/2) = |\overline{df}|\cos\phi \tag{1a}$$

A similar force balance in the $\hat{U}_n$ direction gives

$$T\sin(d\beta/2) - (T + dT)\sin(d\beta/2) = |\overline{df}|\sin\phi \tag{1b}$$

making the substitutions $|\overline{df}| = \omega^2 R\, dm$, $\cos(d\beta/2) = 1$, $\sin(d\beta/2) = d\beta/2$, and noting that $2T + dT = 2T$ in the limit as $dT \to 0$, we get

$$dT = -\omega^2 R\cos\phi\, dm \tag{2a}$$

$$d\beta = \omega^2(R\sin\phi/T)\, dm \tag{2b}$$

In these equations, the variables R, T, ϕ, and β can be expressed as functions of either θ or the accumulated length along the tether from the horizontal axis ℓ. In the latter case, we can write

$$dT/d\ell = -\omega^2 M_d R\cos\phi \tag{3a}$$

and

$$d\beta/d\ell = \omega^2 M_d (R\sin\phi/T) \tag{3b}$$

where $d\ell$ is the differential length along the tether and $M_d = dm/d\ell$ the constant mass density of the tether.

Equations (3) have important physical interpretations as follows. Equation (3a) states that the differential change in tension at any point along the tether is equal to the tangential component of the centrifugal force of the differential mass in that section of the tether. Intuition supports this result and also suggests that this equation must apply to any statics problem in which a distributed force distorts a string under tension.

In Eq. (3b), $d\beta/d\ell$ is the radius of curvature of the tether at that point as radius of curvature is conventionally defined. Therefore, the equation states that the radius of curvature at any point on the tether is directly proportional to the normal component of the centrifugal force acting on the differential element and inversely proportional to the tension at the point. This observation also is intuitively reasonable and applies to any statics problem of this type.

Finally, it is convenient to normalize Eqs. (3) by expressing all distances as a fraction of the tether length L from the horizontal axis to the corner mass, all masses as a fraction of the corner mass M_1, and the tension force as a fraction of the quantity $M_1 L\omega^2$, which has the dimensions of force. This leads to the substitutions $R = LR_n$, $d\ell = L\, d\ell_n$, $T = M_1 L\omega^2 T_n$, and $T = M_1 L\omega^2 dT_n$ into Eqs. (3), where the subscript n stands for normalized quantities

$$dT_n/d\ell_n = -(M_d L/M_1)R_n\cos\phi \tag{4a}$$

$$d\beta/d\ell_n = (M_d L/M_1)R_n\sin\phi/T_n \tag{4b}$$

Note from these equations that neither the normalized shape R_n nor the real shape R is affected by the rotational velocity ω. The normalized tension is also not affected by ω, but the real tension is proportional to ω^2. The only parameters that do affect the normalized shape and tension are the dimensionless quantity $(M_d L/M_1)$, which will be designated the normalized tether mass density (M_{dn}), and the corner masses M_1 and M_2, which determine the boundary conditions.

We can identify two boundary conditions and a third constraint that must also be satisfied by any solution to this problem. At $\theta = 0$, the angles β and ϕ must both equal $\pi/2$ if the mass M_2 is absent, as can be seen in Fig. 1a. If M_2 is present, these angles are determined by the requirement that the tension forces exerted by the two tethers connected to M_2 must balance the centrifugal force of M_2. $2T(0)\cos[\phi(0)] = \omega^2 M_2 R(0)$ or, using normalized quantities and the normalized secondary point mass $M_{2n} = M_2/M_1$,

$$2T_n(0)\cos[\phi(0)] = (M_{2n})\, R_n(0) \tag{5a}$$

at $\theta = \pi/3$. The same force balance is required at M_1, resulting in the following boundary condition:

$$2T_n(\pi/3)\cos[\phi(\pi/3)] = R_n(\pi/3) \tag{5b}$$

The third constraint on the solution is imposed by the fixed length of the tether L which, in terms of normalized variables, requires

$$1 = \int_0^{\pi/3}\left(\frac{d\ell_n}{d\theta}\right)d\theta = \int_0^{\pi/3}\sqrt{\left(\frac{dR_n}{d\theta}\right)^2 + R_n^2}\, d\theta \tag{5c}$$

In view of the highly nonlinear nature of these equations, and in view of the integral contition (5c), it seems unlikely that an exact solution can be found. However, a numerical solution is available as follows.

Algorithm

The iteration procedure starts by dividing the range of θ into $K - 1$ equal segments with step size $\Delta\theta$ as shown in Fig. 2a, where $K = 5$. The discrete versions of Eqs. (4) and boundary conditions (5a) and (5b) are shown below along with the discrete version of condition (5c):

$$\Delta T_n = T_n(k) - T_n(k-1) = M_{dn}\, R_n(k)\cos[\phi(k)]\,\Delta\ell_n(k) \tag{6a}$$

$$\Delta\beta = \beta(k+1) - \beta(k) = M_{dn}\,[R_n(k)/T_n(k)]\sin[\phi(k)]\,\Delta\ell_n(k) \tag{6b}$$

$$\cos[\phi(1)] = 0.5\, M_{2n}\, R_n(1)/T_n(1) \tag{7a}$$

$$T_n(K) = 0.5R_n(K)/\cos[\phi(K)] \tag{7b}$$

$$\sum_{k=2}^{K}\Delta\ell_n(k) = 1 \tag{7c}$$

The two arrays $[R_n(K)]$ and $[T_n(K)]$, which contain the radii and the tensions at each of the K discrete positions along the tether, are the unknowns that must be determined by the iteration method in such a way that they satisfy Eqs. (6) and (7). Although the finite step size introduces an approximation, this problem is overcome easily by making the step size

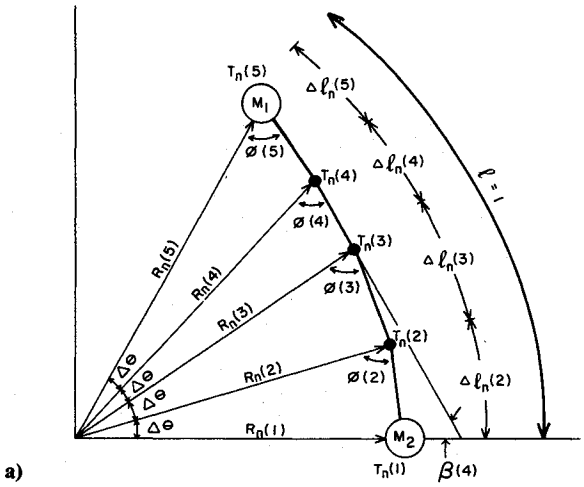

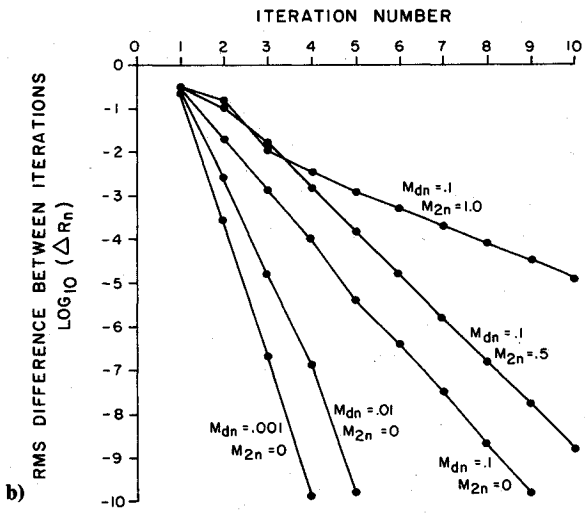

Fig. 2 a) Lumped parameter model used in the algorithm for the case of five lumped masses; and b) plot of the rms difference between iterations against the iteration number for six different combinations of parameter values, showing the rapid convergence of the algorithm.

variable in the computer implementation of the algorithm, and then reducing it as desired.

Observation of Eqs. (6) suggests the following procedure. First, guess a tether "shape" that will determine initial values for R_n, $\Delta\ell_n$, ϕ, and β at each discrete position along the tether. The initial values of R_n are placed in the array $[R_n(K)]_0$, where the subscript 0 designates the zeroth iteration. Then use these values in Eq. (6a) to find the initial array $[T_n(K)]_0$ at each position, sequentially starting at the upper boundary where $T_n(K)_0$ is given by Eq. (7b) and working down from $k = K$ to 1. Next, use all of the zeroth iteration values in Eq. (6b) to find a new angle β at each discrete position by starting at the $k = 1$ boundary value given by Eq. (7a) and working up through $k = K$. The updated "shape" is embodied in this $[\beta(K)]_1$ array, which gives a new curvature at each point. It can be used to update the R_n, $\Delta\ell_n$, ϕ, and β arrays using only geometrical considerations and the total length condition (7c). The updated $[R_n(K)]$ array then can be used to start a new iteration.

This procedure can be repeated indefinitely giving a series of values for $[R_n(K)]_m$, which, it is hoped, will converge as m increases. If it does converge, the result must satisfy Eqs. (6) and (7) and, therefore, must be a solution to the problem. A mathematical proof of convergence is not attempted here, but a computer program implementing the preceding scheme has been observed to converge for all reasonable parameter values and for two very different starting tether shapes. The convergence was measured by taking the rms difference ΔR_n between successive values of the $[R_n(K)]_m$ array, the results of which are shown in Fig. 2b for six combinations of system parameters. Note that the rate of convergence is faster for lower values of the tether mass density and for lower values of the mass M_2.

Now that the statics problem has been solved, it is being used as the starting point in the calculation of the dynamic response of the same system when gravity gradients, solar radiation pressure, atmospheric drag, and thermal expansion forces are present. In turn, this will be used to model a system designed to control the attitudes and positions of the collimating telescopes in the proposed interferometer.

References

[1]Vakili, F., "Triangle: A Different Design for a Three Satellite Interferometer in Space," *ESA, Proceedings of the Colloquium on Kilometric Optical Arrays in Space,* European Space Agency, Noordwijk, The Netherlands, SP-226, April 1985, p. 107.

[2]Crellin, E. B., "Preliminary Studies of a Spinning Tether-Connected Trio Concept," *ESA, Proceedings of the Colloquium on Kilometric Optical Arrays in Space,* European Space Agency, SP-226, April 1985, p. 91.

[3]Goodman, J. W., "Statistical Optics," Wiley, 1985, pp. 207–211.

Generation of Infrared Earth Radiance for Attitude Determination

T. K. Alex* and Ramani Seshamani†
ISRO Satellite Centre, Bangalore, India

Introduction

INFRARED Earth sensors, which detect the infrared horizon of the Earth in the 15 μm carbon dioxide band, determine the roll and pitch errors of the spacecraft.[1] The Earth chord width and the reference time signals synchronized with the scanning are used to derive the attitude errors. Generally, these sensors detect the relative change in the radiation at the horizon by differentiating the preamplified electronic signal from the detector. Since there is a radiance gradient across the Earth, the differentiator output from the Earth sensor will tend to give a constant offset, the sign and the amplitude of which depend upon the direction of the gradient and the slope of the gradient, respectively, the slope being inversely proportional to the angular width of the Earth as seen from the satellite. Whereas for a low-Earth orbiting satellite the offset error is $\approx$0.6 deg, for a geostationary satellite it is $\approx$0.15 deg. Whereas for earlier spacecraft, which had more symmetric configurations and less stringent payload

Received Nov. 5, 1987.

*Head, Sensor Systems Division.
†Engineer, Sensor Systems Division.